Iterative Substructuring Methods for Indoor Air Flow Simulation

Tobias Knopp[1], Gert Lube[1], Ralf Gritzki[2], and Markus Rösler[2]

[1] Georg-August-University of Göttingen, Math. Department, NAM
[2] Dresden University of Technology, Faculty of Mech. Engrg., TGA

Summary. The numerical simulation of turbulent indoor-air flows is performed using iterative substructuring methods. We present a framework for coupling eddy-viscosity turbulence models based on the non-stationary, incompressible, non-isothermal Navier-Stokes problem with non-isothermal near-wall models; this approach covers the k/ϵ model with an improved wall function concept. The iterative process requires the fast solution of linearized Navier-Stokes problems and of advection-diffusion-reaction problems. These subproblems are discretized using stabilized FEM together with a shock-capturing technique. For the linearized problems we apply an iterative substructuring technique which couples the subdomain problems via Robin-type transmission conditions. The method is applied to a benchmark problem, including comparison with experimental data by Tian and Karayiannis [2000] and to realistic ventilation problems.

1 A full-overlapping DDM for wall-bounded flows

Let $\Omega \subset \mathbf{R}^d,\ d = 2, 3$ be a bounded Lipschitz domain. As the basic mathematical model we consider the (non-dimensional) incompressible, non-isothermal Navier-Stokes equations with an eddy-viscosity model to be specified later and the Boussinesq approximation for buoyancy forces. We seek a velocity field $\mathbf{u}$, pressure p, and temperature θ as solutions of

$$\begin{aligned} \partial_t \mathbf{u} - \boldsymbol{\nabla} \cdot (2\nu_e \mathbb{S}(\mathbf{u})) + (\mathbf{u} \cdot \boldsymbol{\nabla})\mathbf{u} + \boldsymbol{\nabla} p &= -\beta\theta\mathbf{g} \\ \boldsymbol{\nabla} \cdot \mathbf{u} &= 0 \\ \partial_t \theta + (\mathbf{u} \cdot \boldsymbol{\nabla})\theta - \boldsymbol{\nabla} \cdot (a_e \boldsymbol{\nabla}\theta) &= \dot{q}^V c_p^{-1} \end{aligned} \tag{1}$$

with $\mathbb{S}(\mathbf{u}) := \frac{1}{2}(\boldsymbol{\nabla}\mathbf{u} + \boldsymbol{\nabla}\mathbf{u}^T)$, isobaric volume expansion coefficient β, gravitational acceleration $\mathbf{g}$, volumetric heat source $\dot{q}^V$, and specific heat capacity (at constant pressure) c_p. Moreover, we introduce effective viscosities $\nu_e = \nu + \nu_t$ and $a_e = a + a_t$ with kinematic viscosity ν, turbulent viscosity ν_t, thermal diffusivity $a = \nu Pr^{-1}$ and turbulent thermal diffusivity $a_t = \nu_t Pr_t^{-1}$ with

Prandtl numbers $Pr = 0.7$ and $Pr_t = 0.9$. Therein, the non-constant ν_t and a_t are supposed to model turbulent effects and are considered in detail later. Depending on the sign of $\mathbf{u} \cdot \mathbf{n}$, the boundary $\partial\Omega$ is divided into wall zones $\Gamma_0 \equiv \Gamma_W$, inlet zones Γ_- and outlet zones Γ_+. We impose

$$\sigma(\mathbf{u}, p)\mathbf{n} = \tau_n \mathbf{n} \quad \text{on } \Gamma_- \cup \Gamma_+ \ , \qquad \mathbf{u} = \mathbf{0} \quad \text{on } \Gamma_0 \tag{2}$$

with $\sigma(\mathbf{u}, p) = 2\nu_e \mathbb{S}(\mathbf{u}) - p\mathbb{I}$. For θ we require

$$\theta = \theta_{in} \quad \text{on } \Gamma_- \ , \quad a_e \boldsymbol{\nabla}\theta \cdot \mathbf{n} = 0 \quad \text{on } \Gamma_+ \ , \qquad \theta = \theta_w \quad \text{on } \Gamma_0. \tag{3}$$

In an outer loop, for the semidiscretization in time we apply the implicit Euler scheme which leads to a sequence of coupled non-linear problems to be solved from time step to time step. Denote $\tilde{\partial}_t \phi = (\phi - \phi^{old})/(\Delta t)$ the backward-difference quotient in time for a certain variable ϕ with time-step Δt.

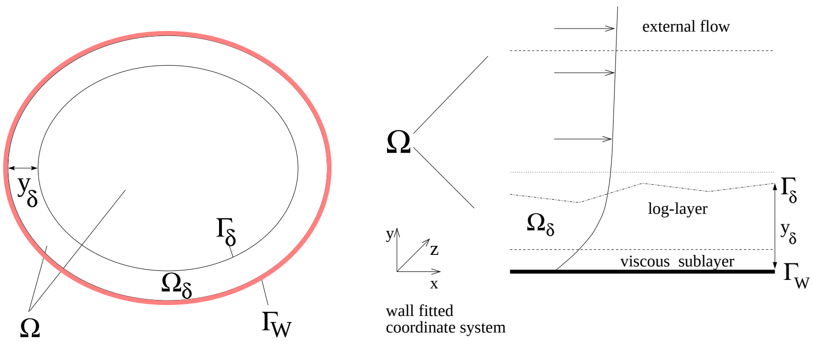

Fig. 1. Domain decomposition in the boundary layer region

Near Γ_W, the solutions for $\mathbf{u}$ and θ often exhibit strong gradients. As an illustration, Fig. 1 (right) shows the typical near-wall profile of the streamwise component of $\mathbf{u}$. The aim is to circumvent an anisotropic grid refinement in the near-wall region, which is computationally very expensive. For this purpose we study an overlapping domain-decomposition method which is presented in the sequel, see also Fig. 1 (left). For clarity of the presentation we assume $\partial\Omega = \Gamma_0 \equiv \Gamma_W$; for the general case we refer to Knopp et al. [2002] and Knopp [2003]. We start with the global problem with modified boundary conditions on Γ_W compared to (2), (3):

$$\begin{aligned}
\tilde{\partial}_t \mathbf{u} - \boldsymbol{\nabla} \cdot (\nu_e \boldsymbol{\nabla}\mathbf{u}) + (\mathbf{u} \cdot \boldsymbol{\nabla})\mathbf{u} + \boldsymbol{\nabla} p &= -\beta\theta\mathbf{g} && \text{in } \Omega \\
\boldsymbol{\nabla} \cdot \mathbf{u} &= 0 && \text{in } \Omega \\
\mathbf{u} \cdot \mathbf{n} = 0 \ , \qquad (\mathbb{I} - \mathbf{n} \otimes \mathbf{n})\sigma(\mathbf{u}, p)\mathbf{n} &= \boldsymbol{\tau}_t(\mathbf{u}, \mathbf{u}^{BL}, \theta^{BL}) && \text{on } \Gamma_W \\
\tilde{\partial}_t \theta + (\mathbf{u} \cdot \boldsymbol{\nabla})\theta - \boldsymbol{\nabla} \cdot (a_e \boldsymbol{\nabla}\theta) &= \dot{q}^V c_p^{-1} && \text{in } \Omega \\
a_e \boldsymbol{\nabla}\theta \cdot \mathbf{n} &= \dot{q}(\mathbf{u}^{BL}, \theta^{BL}) c_p^{-1} && \text{on } \Gamma_W
\end{aligned} \tag{4}$$

where the r.h.s. data $\boldsymbol{\tau}_t(\mathbf{u}, \mathbf{u}^{BL}, \theta^{BL})$, $\dot{q}(\mathbf{u}^{BL}, \theta^{BL})$ are determined from

$$\begin{aligned}
\tilde{\partial}_t \mathbf{u}^{BL} - \boldsymbol{\nabla} \cdot (\nu_e^{BL} \boldsymbol{\nabla} \mathbf{u}^{BL}) + (\mathbf{u}^{BL} \cdot \boldsymbol{\nabla}) \mathbf{u}^{BL} + \boldsymbol{\nabla} p^{BL} &= \mathbf{f} && \text{in } \Omega_\delta \\
\boldsymbol{\nabla} \cdot \mathbf{u}^{BL} &= 0 && \text{in } \Omega_\delta \\
\mathbf{u}^{BL} = \mathbf{0} \quad \text{on } \Gamma_W, \qquad \mathbf{u}^{BL} &= \mathbf{u} && \text{on } \Gamma_\delta \qquad (5) \\
\tilde{\partial}_t \theta^{BL} + (\mathbf{u}^{BL} \cdot \boldsymbol{\nabla}) \theta^{BL} - \boldsymbol{\nabla} \cdot (a_e^{BL} \boldsymbol{\nabla} \theta^{BL}) &= \dot{q}^V c_p^{-1} && \text{in } \Omega_\delta \\
\theta^{BL} = \theta_w \quad \text{on } \Gamma_W, \qquad \theta^{BL} &= \theta && \text{on } \Gamma_\delta .
\end{aligned}$$

Now we specify ν_t, $\boldsymbol{\tau}_t(\mathbf{u}, \mathbf{u}^{BL}, \theta^{BL})$, $\dot{q}(\mathbf{u}^{BL}, \theta^{BL})$ in (4), and we modify (5).
(I) Global turbulence model in Ω: In (4), as a particular but successful choice for indoor-air flow simulation, we apply the k/ϵ model for ν_t (see, e.g., Codina and Soto [1999]) using the formula $\nu_t = c_\mu k^2 \epsilon^{-1}$ ($c_\mu = 0.09$) with turbulent kinetic energy k and turbulent dissipation ϵ being the solution of

$$\begin{aligned}
\tilde{\partial}_t k + (\mathbf{u} \cdot \boldsymbol{\nabla}) k - \boldsymbol{\nabla} \cdot (\nu_k \boldsymbol{\nabla} k) &= P_k + G - \epsilon \qquad (6) \\
\tilde{\partial}_t \epsilon + (\mathbf{u} \cdot \boldsymbol{\nabla}) \epsilon - \boldsymbol{\nabla} \cdot (\nu_\epsilon \boldsymbol{\nabla} \epsilon) + C_2 \epsilon^2 k^{-1} &= C_1 \epsilon k^{-1} (P_k + G)
\end{aligned}$$

with constants $C_1 = 1.44, C_2 = 1.92, Pr_k = 1.0, Pr_\epsilon = 1.3$, effective viscosities $\nu_k = \nu + \nu_t Pr_k^{-1}, \nu_\epsilon = \nu + \nu_t Pr_\epsilon^{-1}$, production and buoyancy terms

$$P_k := 2\nu_t |\mathbb{S}(\mathbf{u})|^2, \quad G := C_t \beta a_t \mathbf{g} \cdot \boldsymbol{\nabla} \theta \ , \quad C_t = 0.8.$$

The k/ϵ-equations (6) are solved in $\Omega \backslash \Omega_\delta$ with the following boundary conditions (with $\kappa = 0.41$ and $U_* = |\boldsymbol{\tau}_t|^{1/2}$)

$$k = c_\mu^{-1/2} U_*^2, \qquad \epsilon = U_*^3 / (\kappa y) \ \text{ on } \Gamma_\delta .$$

Alternatively to (6), we can use an eddy-viscosity-based LES model for ν_t in Ω, e.g., the non-isothermal *Smagorinsky model* with Eidson's modification

$$\nu_t = (C_S \Delta)^2 \left(\max\{ \ 0 \ ; \ ||\mathbb{S}(\mathbf{u})||_F^2 + \frac{\beta}{Pr_t} \mathbf{g} \cdot \boldsymbol{\nabla} \theta \} \right)^{1/2}, \ a_t = \frac{\nu_t}{Pr_q}$$

with $C_S = 0.21$ and $Pr_q = 0.04$.
(II) Boundary layer model in Ω_δ: Denote x, y, z the streamwise, wall-normal and spanwise direction resp. in a wall-fitted coordinate system, see Fig. 1 (right). We simplify (5) in Ω_δ under standard assumptions in Prandtl's boundary layer theory (cf. Knopp [2003]) and using modified effective viscosities in Ω_δ

$$\nu_e^{BL} = \nu \max \left(1; \frac{Re}{Re_{min}} \right), \quad a_e^{BL} = \frac{\nu}{Pr} \max \left(1; \frac{Pr}{Pr_t^{BL}} \frac{Re}{Re_{min}} \right) \qquad (7)$$

with $Re(x, y, z) = |\mathbf{u}^{BL}(x, y, z)| y / \nu$, $Pr_t^{BL} = 1.16$ and with the following empirical formula which accounts for effects of thermal stratification in the boundary layer, see Knopp [2003] and references therein, viz.,

$$Re_{min} = R_0 \min[\exp(-K_s \dot{q} Pr \nu U_*^{-4} \mathbf{g} \cdot \mathbf{n}); 70], \; R_0 = 20.0, \; K_s = 25.0. \quad (8)$$

Then, instead of a set of partial differential equations (5), in Ω_δ we solve

$$\begin{aligned} -\frac{d}{dy}\left(\nu_e^{BL} \frac{du_x^{BL}}{dy}\right) &= -\beta \theta^{BL} g_x, \\ -\frac{d}{dy}\left(a_e^{BL} \frac{d\theta^{BL}}{dy}\right) &= 0, \\ u_x^{BL}|_{y=0} = 0 \; , \qquad \theta^{BL}|_{y=0} &= \theta_w, \end{aligned} \quad (9)$$

with g_x being the streamwise component of $\mathbf{g}$ and matching conditions

$$u_x^{BL}|_{y=y_\delta} = u_x(y_\delta), \qquad \theta^{BL}|_{y=y_\delta} = \theta(y_\delta). \quad (10)$$

Now we decouple and linearize the model (I), (II) within each time step:

(A) First update ν_t, a_t. Then update $\boldsymbol{\tau}_t$, $\dot{q}$: Given u_x, θ on Γ_δ from the previous iteration cycle, we replace the boundary condition (10) with

$$\nu_e \frac{du_x^{BL}}{dy}|_{y=0} = R, \qquad a_e \frac{d\theta^{BL}}{dy}|_{y=0} = S. \quad (11)$$

and solve the initial value problem (7),(8),(9),(11) using a shooting method for (R, S) until the conditions (10) are fulfilled. Then we find the r.h.s. $\boldsymbol{\tau}_t = -U_*^2 \mathbf{u}/||\mathbf{u}||$ and $\dot{q}$ in (4) by setting $U_*^2 = R$ and $\dot{q} = c_p S$.

(B) We solve (4) and, if the k/ϵ model is used for ν_t, additionally (6), using a block Gauss-Seidel method.

(C) If a certain stopping-criterion is not yet fulfilled, then goto step (A). Otherwise goto next time step.

Step (B) requires the solution of two basic problems. First, the linearized equations for θ, k and ϵ are *advection-diffusion-reaction* (ADR) problems with non-constant viscosity of the general form (skipping the restriction $\partial\Omega = \Gamma_0$):

$$\begin{aligned} Lu \equiv -\boldsymbol{\nabla} \cdot (\nu \boldsymbol{\nabla} u) + (\mathbf{b} \cdot \boldsymbol{\nabla}) u + cu &= f && \text{in } \tilde{\Omega} \\ u &= g && \text{on } \tilde{\Gamma}_D \\ \nu \boldsymbol{\nabla} u \cdot \mathbf{n} &= h && \text{on } \tilde{\Gamma}_N. \end{aligned} \quad (12)$$

Secondly, the linearized Navier-Stokes equations are of *Oseen*-type with a positive reaction term and non-constant viscosity:

$$\begin{aligned} L_O(\mathbf{a}, \mathbf{u}, p) \equiv -\boldsymbol{\nabla} \cdot (2\nu \mathbb{S}(\mathbf{u})) + (\mathbf{a} \cdot \boldsymbol{\nabla})\mathbf{u} + c\mathbf{u} + \boldsymbol{\nabla} p &= \mathbf{f} && \text{in } \Omega \\ \boldsymbol{\nabla} \cdot \mathbf{u} &= 0 && \text{in } \Omega \\ \sigma(\mathbf{u}, p)\mathbf{n} &= \tau_n \mathbf{n} && \text{on } \Gamma_- \cup \Gamma_+ \\ (\mathbb{I} - \mathbf{n} \otimes \mathbf{n})\sigma(\mathbf{u}, p)\mathbf{n} = \boldsymbol{\tau}_t, \qquad \mathbf{u} \cdot \mathbf{n} &= 0 && \text{on } \Gamma_0. \end{aligned} \quad (13)$$

For the finite element discretization of (12)-(13) we assume an admissible triangulation $\mathcal{T}_h = \{K\}$ of Ω and define discrete subspaces $X_h^l \equiv \{v \in C(\overline{\Omega}) \mid v|_K \in \Pi_l(K)\ \forall K \in \mathcal{T}_h\},\ l \in \mathbf{N}$.
For the ADR-problem (12), for simplicity with $g = 0$ on Γ_D, we apply the Galerkin-FEM with SUPG-stabilization:

$$\text{Find } u \in V_h = \{v \in X_h^l \mid v|_{\Gamma_D} = 0\} \text{ s.t. : } b^s(u,v) = l^s(v) \quad \forall v \in V_h \ , \quad (14)$$

$$b^s(u,v) = (\nu \boldsymbol{\nabla} u, \boldsymbol{\nabla} v)_\Omega + ((\mathbf{b} \cdot \boldsymbol{\nabla})u + cu, v)_\Omega + \sum_{T \in \mathcal{T}_h} (\delta_T L u, (\mathbf{b} \cdot \boldsymbol{\nabla})v)_T$$
$$l^s(v) = (f,v)_\Omega \ + \ (h,v)_{\Gamma_N} + \sum_{T \in \mathcal{T}_h} (\delta_T f, (\mathbf{b} \cdot \boldsymbol{\nabla})v))_T$$

where $(\cdot,\cdot)_S$ denotes the inner product on some S and with an appropriate parameter set $\{\delta_T\}_T$, see Knopp et al. [2002]. Additionally, we use a (nonlinear) shock-capturing method, see Knopp et al. [2002].
For the Oseen problem (13), we define the discrete spaces $\mathbf{V}_h \times Q_h = (X_h^r)^d \times X_h^s$ with $r, s \in \mathbf{N}$. The Galerkin FEM reads:

$$\text{Find } U = (\mathbf{u}, p) \in \mathbf{V}_h \times Q_h, \text{ s.t. } \mathcal{A}(U,V) = \mathcal{L}(V)\ \forall\, V = (\mathbf{v}, q) \in \mathbf{V}_h \times Q_h \quad (15)$$

with the (bi)linear forms

$$\mathcal{A}(U,V) = a(\mathbf{u},\mathbf{v}) + b(\mathbf{v},p) - b(\mathbf{u},q) \ , \qquad b(\mathbf{v},p) = -(p, \boldsymbol{\nabla} \cdot \mathbf{v}),$$
$$a(\mathbf{u},\mathbf{v}) = (2\nu \mathbb{S}(\mathbf{u}), \boldsymbol{\nabla} \mathbf{v})_\Omega + ((\mathbf{a} \cdot \boldsymbol{\nabla})\mathbf{u} + c\mathbf{u}, \mathbf{v})_\Omega - (\mathbf{n} \otimes \mathbf{n} \sigma(\mathbf{u},p)\mathbf{n}, \mathbf{v})_{\Gamma_0}$$
$$\mathcal{L}(V) = (\mathbf{f}, \mathbf{v})_\Omega + (\tau_n \mathbf{n}, \mathbf{v})_{\Gamma_- \cup \Gamma_+} + (\boldsymbol{\tau}_t, \mathbf{v})_{\Gamma_0}.$$

Here we use an equal-order ansatz in $\mathbf{V}_h \times Q_h$ ($r = s = 1$); thus the discrete inf-sup condition is not satisfied. As a remedy we apply a pressure stabilization (PSPG) together with divergence and SUPG stabilizations, cf. Knopp et al. [2002].

2 Domain decomposition of the linearized problems

A nonoverlapping domain decomposition method with Robin interface conditions is applied to the basic linearized problems (12), (13). Consider a nonoverlapping partition of Ω (which, for simplicity, is assumed to be stripwise) into convex, polyhedral subdomains being aligned with the FE mesh, i.e.

$$\overline{\Omega} = \cup_{k=1}^N \overline{\Omega}_k, \quad \Omega_k \cap \Omega_j = \emptyset \quad \forall k \neq j \ , \quad \forall K \in \mathcal{T}_h \ \exists k \ : \ K \subset \Omega_k.$$

Moreover, we set $\Gamma_{jk} := \partial\Omega_j \cap \partial\Omega_k,\ j \neq k$, with $\Gamma_{kj} \equiv \Gamma_{jk}$.
For the (continuous) ADR-problem (12) the DDM reads: for given u_k^n from iteration step n on each Ω_k, seek (in parallel) for u_k^{n+1}

$$\begin{aligned} Lu_k^{n+1} &= f && \text{in } \Omega_k \\ u_k^{n+1} &= 0 && \text{on } \Gamma_D \cap \partial\Omega_k \\ \nu \boldsymbol{\nabla} u_k^{n+1} \cdot \mathbf{n}_k &= h && \text{on } \Gamma_N \cap \partial\Omega_k \end{aligned} \tag{16}$$

together with the interface conditions (with a relaxation parameter $\theta \in (0, 1]$)

$$\begin{aligned} \Phi_k(u_k^{n+1}) &= \theta\Phi_k(u_j^n) + (1-\theta)\Phi_k(u_k^n) \quad \text{on } \Gamma_{jk},\ j = 1, \dots, N,\ j \neq k \\ \Phi_k(u) &= \nu \boldsymbol{\nabla} u \cdot \mathbf{n}_k + (-\frac{1}{2}\mathbf{b} \cdot \mathbf{n}_k + z_k)u. \end{aligned} \tag{17}$$

Let $V_{k,h}$, b_k^s, and l_k^s denote the restrictions of V_h, b^s, and l^s to a subdomain Ω_k. Moreover, $W_{kj,h}$ is the restriction of V_h to the interface part Γ_{kj}. The inner product in $L^2(\Gamma_{kj})$ or, whenever needed, the dual product in $(W_{kj,h})^* \times W_{kj,h}$ is denoted by $\langle \cdot, \cdot \rangle_{\Gamma_{kj}}$.

The *fully discretized* DDM reads for $k = 1, \dots, N$ and given u_k^n, Λ_{jk}^n:

Parallel computation step: find $u_k^{n+1} \in V_{k,h}$ s.t. $\forall\ v_k \in V_{k,h}$

$$b_k^s(u_k^{n+1}, v_k) + \langle (-\frac{1}{2}\mathbf{b} \cdot \mathbf{n}_k + z_k)u_k^{n+1}, v_k \rangle_{\Gamma_{kj}} \ = \ l_k^s(v_k) + \sum_{j(\neq k)} \langle \Lambda_{jk}^n, v_k \rangle_{\Gamma_{kj}}.$$

Communication step: for all $j \neq k$, update the Lagrangian multipliers

$$\langle \Lambda_{kj}^{n+1}, \phi \rangle_{\Gamma_{kj}} = \langle \theta(z_k + z_j)u_k^{n+1} - \theta\Lambda_{jk}^n + (1-\theta)\Lambda_{kj}^n, \phi \rangle_{\Gamma_{kj}} \quad \forall \phi \in W_{kj,h}.$$

In Knopp et al. [2002], the analysis of the method is resumed and the following design of the interface function is proposed (motivated by an *a-posteriori estimate*)

$$\begin{aligned} z_k &= \frac{1}{2}|\mathbf{b} \cdot \mathbf{n}_k| + R_k(H), \\ R_k(H) &\sim \frac{\nu_{min}}{H}\left[1 + H\sqrt{\frac{c_{max}}{\nu_{min}}} + \min\left(\frac{H\|\mathbf{b}\|_{max}}{\nu_{min}}; \frac{\|\mathbf{b}\|_{max}}{\sqrt{(\nu c)_{min}}}\right)\right], \end{aligned} \tag{18}$$

with H being the diameter of the interface. A further improvement is achieved with a multilevel type approach with appropriate change of $R_k(\cdot)$ corresponding to higher frequencies of the error, for details see Lube et al. [2003].

For the Oseen problem (13) we proceed similar to the method (16) for the ADR problem. We use the interface conditions

$$\Phi_k(\mathbf{u}_k^{n+1}, p_k^{n+1}) \ = \ \theta\Phi_k(\mathbf{u}_j^n, p_j^n) + (1-\theta)\Phi_k(\mathbf{u}_k^n, p_k^n) \ \text{ on } \Gamma_{jk}.$$

with relaxation parameter $\theta \in (0, 1]$ and the interface function

$$\Phi_k(u, p) = \nu \boldsymbol{\nabla} \mathbf{u} \cdot \mathbf{n}_k - p\mathbf{n}_k + (-\frac{1}{2}\mathbf{a} \cdot \mathbf{n}_k + z_k)\mathbf{u} \tag{19}$$

with acceleration parameter z_k which has the same structure as in (18). Concerning the corresponding parallel algorithm (in weak form), its analysis and further details, we refer to Knopp et al. [2002] and references therein.

3 Application to Indoor Air Flow Simulation

The approach is applied to a standard benchmark test case for indoor-air flow simulation, viz., turbulent natural convection in an air-filled square cavity as sketched in Fig. 2 (left), using the research code *Parallel NS*. Let a tilde denote dimensional quantities. Denote $\tilde{\Omega} = (0, \tilde{H})^3$ with $\tilde{H} = 0.75m$. We impose $\tilde{\theta}_w = 323.15K$ on Γ_h and $\tilde{\theta}_w = 283.15K$ on Γ_c. On $\Gamma_b \cup \Gamma_t$, alternatively, *(i)* we impose θ_w using the experimental data given in Tian and Karayiannis [2000] or *(ii)* we simply require that $a_e \boldsymbol{\nabla}\theta \cdot \mathbf{n} = 0$. Moreover, we have $\tilde{\nu} = 1.53{\times}10^{-5} m^2 s^{-1}$, $\tilde{\beta} = 3.192{\times}10^{-3} K^{-1}$, $\tilde{g} = 9.81 m s^{-2}$, thus giving a Rayleigh number $Ra = \tilde{g}\tilde{\beta}(\tilde{\theta}_h - \tilde{\theta}_c)\tilde{H}^3 Pr/\tilde{\nu} = 1.58 \times 10^9$. We used a structured mesh

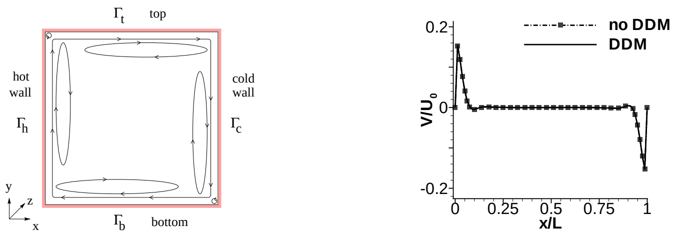

Fig. 2. Sketch of cavity and flow (left) and prediction for V/U_0 at $y/H = 0.5$ (right)

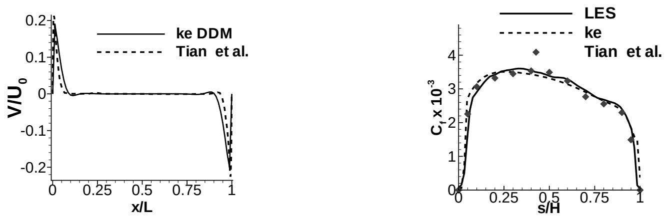

Fig. 3. V/U_0 at $y/H = 0.5$ (left) and $C_f = 2U_*^2/U_0^2$ (right) for variant (i)

with $81 \times 65 \times 29$ grid points being equidistantly distributed in each coordinate direction and we use $\Delta\tilde{t} = 1.0$ for the time step. Computations were performed on a cluster of 4 COMPAQ Professional Workstations XP1000 (667 MHz) connected by Ethernet. Parallelization is accomplished using a master/slave paradigm in the PVM configuration. No coarse-grid solver is used so far.

First, the agreement of the solution with DDM (using a coarse-granular $2 \times 2 \times 1$ partition of Ω) and without DDM (for variant *(ii)*) is obvious, see Fig. 2 (right). Therein, V denotes the streamwise component of $\mathbf{u}$ and $\tilde{U}_0 = 0.9692$. The parallel speed-up achieved was 3.7. The accuracy of the approach (for variant *(i)*) is validated by reference to the experimental data by Tian and Karayiannis [2000]. Fig. 3 (left) shows the k/ϵ model prediction (with DDM) for V. Fig. 3 (right) gives the predictions for $C_f \equiv 2U_*^2/\tilde{U}_0$ on Γ_h with $s \equiv y$ (k/ϵ with DDM for a $2 \times 2 \times 1$ partition, LES model (7) without DDM).

The method is applied at Dresden University as an analysis tool for the design

and investigation of natural ventilation systems, see Richter et al. [2003]. Note that for the simulation presented in Fig. 4, the DDM described in Sec.2 is applied where one subdomain is used for the room and one for the surrounding air with the interface being located in the window.
Summarizing, in this paper we combined two DD strategies for turbulent flows, one for near-wall modelling and one for parallel computation of the linearized problems. For this approach, we demonstrated both the accuracy for a benchmark problem and the applicability to a real-life problem.

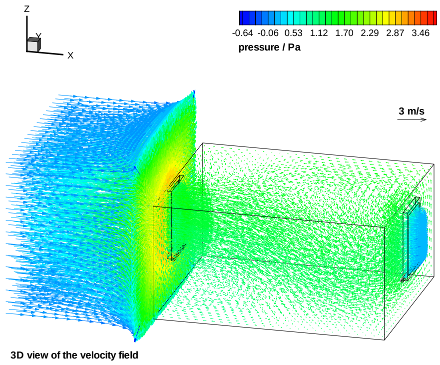

Fig. 4. Indoor-air flow simulation for natural building ventilation.

References

R. Codina and O. Soto. Finite element implementations of two-equation and algebraic stress turbulence models for steady incompressible flow. *Intern. J. Numer. Meths. Fluids*, 90(3):309–334, 1999.

T. Knopp. *Finite-element simulation of buoyancy-driven turbulent flows.* PhD thesis, Universität Göttingen, 2003.

T. Knopp, G. Lube, R. Gritzki, and M. Rösler. Iterative substructuring techniques for incompressible nonisothermal flows and its application to indoor air flow simulation. *Intern. J. Numer. Meths. Fluids*, 40:1527–1538, 2002.

G. Lube, T. Knopp, and G. Rapin. Acceleration of an iterative substructuring method for singularly perturbed elliptic problems. Technical report, Universität Göttingen, 2003.

W. Richter, J. Seifert, R. Gritzki, and M. Rösler. Bestimmung des realen Luftwechsels bei Fensterlüftung aus energetischer und bauphysikalischer Sicht. Technical report, Dresden University of Technology, 2003.

Y. Tian and T. Karayiannis. Low turbulence natural convection in an air filled square cavity, part i: The thermal and fluid flow field. *Int. J. Heat Mass Transfer*, 43:849–866, 2000.